

PRE-ALPINE AND ALPINE DEVELOPMENTS OF THE AUSTRIDIC BASEMENT IN THE SOPRON AREA (EASTERN ALPS, HUNGARY)

GYÖNGYI LELKES-FELVÁRI

Hungarian Geological Institute, Népstadion 14, Budapest

FRANCESCO PAOLO SASSI, DARIO VISONÀ

Istituto di Mineralogia e Petrologia dell'Università, corso Garibaldi 36, 35100 Padova

RIASSUNTO. — Il basamento cristallino dell'area di Sopron (Ungheria) appartiene alla parte più orientale del basamento austridico delle Alpi Orientali. La sua litologia comprende gneiss acidi e rocce simili, metapeliti e metasemipeliti, anfiboliti e quarziti. Nella vicina area del Lago Fertő le anfiboliti sono nettamente prevalenti, e ai litotipi prima elencati si aggiungono filladi e marmi. Come nel rimanente Austroalpino, il carattere polimetamorfico del complesso era già stato messo in evidenza da precedenti autori.

I nuovi dati acquisiti sono congruenti con una evoluzione metamorfica in tre stadi distinti: Alpino, Ercinico, e verosimilmente « Caledoniano » il più antico.

Il metamorfismo più antico (« Caledoniano »?) è responsabile della cristallizzazione dei minerali più vecchi che possono essere individuati mediante l'analisi microstrutturale nelle metapeliti di Sopron. Si tratta di porfiroblasti di staurolite, cianite e granato, ai quali si aggiunge talora sillimanite fibrolitica. Le associazioni mineralogiche indicano quindi per questo evento pre-ercinico condizioni fisiche da facies delle anfiboliti ad almandino, correlate ad un gradiente termico inferiore a 34° C/km.

Gli effetti del metamorfismo ercinico sono variabili da un affioramento all'altro. Il grado metamorfico più elevato è stato trovato nell'area di Brennbergbanya con abbondanti sillimanite ed andalusite, alle quali si associano probabile cordierite e, forse, granato; sono altresì comuni leucosomi di composizione granitica. Altrove il metamorfismo ercinico si presenta con tipici effetti retrogradi, quali la trasformazione dei porfiroblasti di staurolite e di cianite in aggregati di sericite ± clorite ± opachi. Alcuni grandi cristalli di cloritoide, la locale trasformazione di staurolite in cloritoide e la sporadica cloritizzazione dei porfiroblasti di granato possono anche essere tentativamente riferiti a questo evento.

Dagli effetti sopra descritti si deduce che il metamorfismo ercinico abbraccia in quest'area un ampio intervallo di temperature (per lo più facies scisti

verdi e localmente facies anfibolitica) ed è legato ad un gradiente termico maggiore di 34° C/km.

Effetti termicamente congruenti a quelli ercinici sopra descritti si riscontrano nei metagraniti biotitici, nelle metavulcaniti e metavulcanoclastiti acide e negli gneiss chiari. La loro età però può essere sia ercinica che alpina.

I più importanti effetti del metamorfismo alpino sono ben riconoscibili. I più tipici sono: piccoli idioblasti di cloritoide e di cianite per lo più localizzati negli aggregati sericitici, rari idioblasti di staurolite aventi la stessa localizzazione e, forse, piccoli idioblasti di granato. A questo evento sono pure riconducibili le associazioni mineralogiche contenenti leuchtenbergite caratteristiche dei livelli di leucofilliti e delle associate quarziti. Le condizioni fisiche della rielaborazione metamorfica alpina corrispondono in generale alla facies degli scisti verdi; solo localmente si sono avute temperature che hanno determinato la cristallizzazione di Festaurolite. Il gradiente termico alpino fu inferiore ai 34° C/km, come mostrato dalla stabilità della cianite.

Nel quadro sopra esposto è stata menzionata solo la cristallizzazione di minerali petrologicamente importanti dei tre stadi metamorfici riconosciuti nel basamento di Sopron. È ovvio, comunque, che in ciascuno stadio siano cristallizzati anche altri minerali, come imposto dalle pertinenti condizioni fisiche.

La storia metamorfica sopra delineata per l'area di Sopron concorda perfettamente con quella del basamento austridico affiorante più ad occidente nelle Alpi Orientali.

ABSTRACT. — The present paper gives a petrographic characterization of the main rock types outcropping in the Sopron area, in such a way that the data can easily be integrated within the frame of literature on the Eastern Alps. Geothermometric and geobarometric estimations are proposed, based on a multistage interpretation of

the metamorphic evolution of these rocks, as suggested by microtextural analysis. An evolutionary model for this basement is proposed, distinguishing pre-Alpine from Alpine effects. The pre-Alpine metamorphic development of these rocks is interpreted as due to the overprint of the Hercynian on the «Caledonian» event. The compositional features (microprobe analyses) of several minerals integrate the petrologic picture.

Introduction

The crystalline basement in the Sopron area (Western Hungary) belongs to the easternmost part of the Austridic basement of the Eastern Alps (fig. 1). It is covered by Miocene and Pliocene sediments.

The main features of this basement were described by VENDEL (1973), VENDEL et al. (1974) and KISHÁZI (1977) and in numerous internal reports of the Research Institute for Mining (Sopron). The above authors recognized the polymetamorphic character of these rocks, and related them to the «Grobgnéis Serie» outcropping in neighbouring areas in Austria.

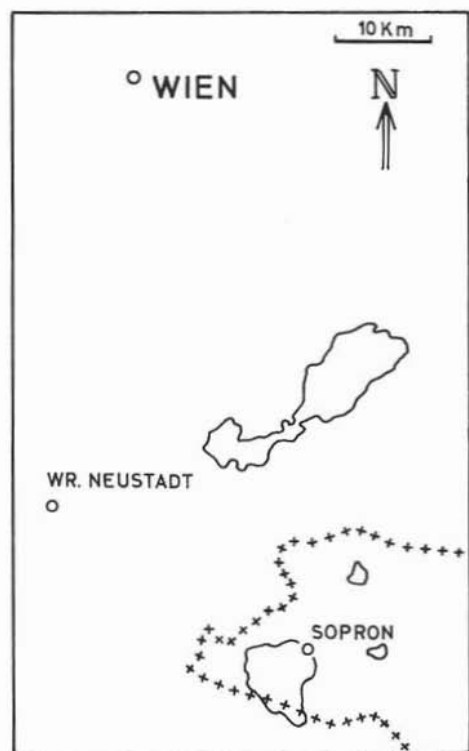


Fig. 1. — Sketch showing the location of the area.

Similar basement rocks outcrop a few kilometers to the north, close to Lake Fertő. Known in the literature as the Fertőrákos basement, it is characterized by the fact that phyllites and marbles also occur and amphibolites prevail. According to KÓSA & FAZEKAS (1982), the Fertőrákos rocks may be correlated with the Wechsel Series.

The opportunity of correlating the Sopron basement with the Austridic basement rocks outcropping further to the west in Austria and Italy, and the need to unravel its complex history, trying to separate Alpine from pre-Alpine effects and compare them with those recognized in the Austrian and Italian parts of the Austrides, were the main reasons for the present research. A first attempt in this direction was made in 1981 by LELKES & SASSI. The main aims of the present, more extensive attempt are:

(1) to outline suitable petrographic characters of the main rock types, so that data may easily be integrated within the frame of Eastern Alpine literature;

(2) where possible, to attempt geothermometric and geobarometric interpretation of petrographic data;

(3) to propose an evolutionary model for this basement distinguishing the pre-Alpine from the Alpine development stage;

(4) to integrate this evolutionary model in the frame of regional knowledge.

Considering that the Fertőrákos basement is mainly known only from drillings, since outcrops are very poor, the present research is mostly based on data from the Sopron area, where the following main rock types outcrop:

- 1) acidic gneisses and related rocks;
- 2) metapelites, metasemipelites and related rocks;
- 3) amphibolites.

Although quartzites also occur, they cannot contribute significant information to the above four goals, and were therefore disregarded in the present stage of our research. On the other hand, leuchtenbergite-bearing rocks are considered separately (LELKES et al., 1983).

1. Acidic gneisses and related rocks

Acidic rocks of various types occur frequently in the Sopron area, and have been described in the literature as orthogneisses, aplitic gneisses, injected gneisses, etc.

Consideration of some compositional and textural features and their combinations is a suitable tool for the simple classification of all these acidic rocks. These features are:

- pre-metamorphic layering;
- pre-metamorphic massive texture;
- strongly hyalal heteroblastic texture;
- occurrence of xenoliths;
- migmatitic texture;
- typical occurrence of biotite;
- typical lack of biotite.

Based on the various combinations of the above features, the following main rock groups have been distinguished:

- biotite-bearing metagranites (features *b*, *c*, *f*);
- acidic metavolcanics and related metavolcanoclastics (features *a*, *c*, *g*);
- biotite-free white gneisses, very probably representing acidic metavolcanics and metavolcanoclastics (features *a*, *g*);
- leucosomes (feature *e*).

This classification is also supported to some extent by chemical features.

1.1. Biotite-bearing metagranites and related blastomylonites

These rocks are known from a quarry (Váris) in the town of Sopron. Similar rocks are also found in the Fertőrákos area, mainly in boreholes. They display very poorly defined foliation as a consequence of the small amount of mica flakes — randomly oriented and scattered in the rock — and the large grain size (1-2 cm). Small elongated xenoliths (a few tens of centimetres) are relatively frequent and mainly consist of biotite and euhedral garnet crystals.

The mineral composition of the metagranites is given by quartz, K-feldspar, plagioclase, biotite, and muscovite. The occurrence of small amounts of garnet is very significant. Apatite is the main accessory mineral.

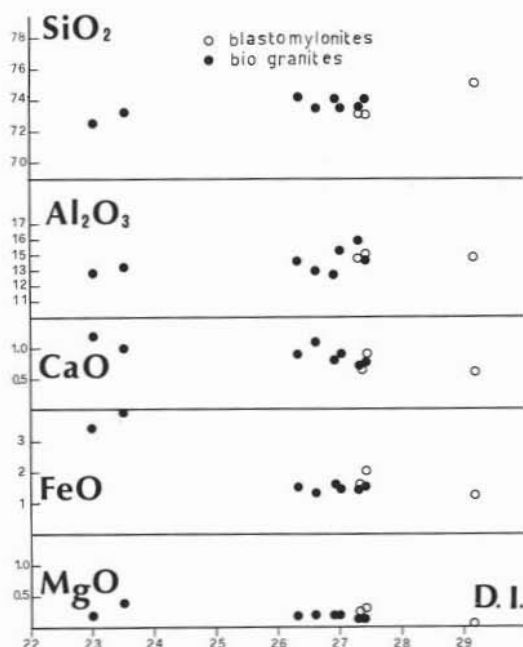


Fig. 2. — Variation diagrams concerning some chemical contents in the biotite-bearing metagranites and in the blastomylonites.

Quartz makes up polycrystalline aggregates which include biotite and apatite.

Potassium feldspar is commonly perthitic, occurring as variously-sized xenoblasts and large subhedral crystals, the latter commonly twinned and including euhedral plagioclase crystals, biotite, quartz, and ores.

Plagioclase occurs as xenoblasts and larger subhedral crystals. The latter represent strongly recrystallized, premetamorphic crystals, as shown by the occurrence in them of abundant sericite and epidote microliths. This occurrence is very typical, and clearly controlled in some cases by the old, now obliterated, zoning of the plagioclase crystals. Plagioclase also includes quartz drops, strongly corroded white mica flakes, and euhedral garnet crystals.

Biotite makes up large flakes, which are sometimes interlayered in white mica flakes, both corroded by quartz and feldspar. Furthermore, biotite locally makes up roughly prismatic aggregates with decussate texture. The biotite rims are commonly marked by a black dust of ores, indicating late compositional alteration of the former biotite. If this fact is disregarded, biotite

TABLE 1
Microprobe analyses of the garnets from biotite-bearing metagranites

	1	2	3	4	5	6	7	8	9	10	11	12	13	14
	47 ₉₁	47 ₉₂	47 ₉₃	48 _{9b2}	48 _{9b1}	49 ₉₁	49 ₉₂	49 _{a1}	49 _{a2}	41 ₉₁	41 ₉₂	41 ₉₃	48 _{9a1}	48 _{9a}
	core	rim				core	rim	core	rim	core	rim		core	rim
SiO ₂	38,74	38,62	38,74	37,77	37,71	38,98	38,92	39,50	39,04	39,30	38,49	39,17	38,28	38,53
TiO ₂	0,0	0,04	0,0	0,0	0,0	0,0	0,08	0,0	0,0	0,01	0,0	0,0	0,0	0,10
Al ₂ O ₃	21,03	21,24	21,06	21,18	20,62	20,97	21,23	21,84	22,09	21,15	21,54	21,35	21,17	21,30
FeO	19,81	19,76	18,77	20,89	12,49	17,18	18,99	19,97	19,74	17,94	17,56	16,51	18,48	19,70
MnO	3,16	4,44	2,61	1,18	4,64	2,49	2,09	3,47	3,21	5,46	5,39	6,40	4,67	1,65
MgO	0,0	0,12	0,0	0,0	0,0	0,1	0,0	0,0	0,11	0,0	0,0	0,05	0,13	0,0
CaO	16,39	15,65	17,67	17,48	22,21	18,26	17,79	15,47	15,96	14,63	15,53	16,51	16,50	17,38
Alm	45	44	43	47	27	40	43	46	45	42	41	37	41,5	45
Prp	-	0,5	-	-	-	0,4	-	-	0,5	-	-	0,2	0,5	-
Spss	7	10	6	3	10	5,6	5	8	7	13	13	15	11	4
Grs	48	45,5	52	50	63	54	52	46	47,5	45	46	47,8	47	51

seems to be stable in the present mineral assemblage.

White mica occurs as large flakes or aggregates with decussate texture. These aggregates are sometimes roughly prismatic in shape, suggesting that they represent pseudomorphs after a prismatic mineral of which no relics have been found. The replaced prismatic mineral was presumably an iron-bearing phase, as the concentration of

numerous fine-grained ores in the white mica aggregates suggest. Large flakes of white mica with opacitic S_1 are occasionally observed.

Garnet occurs in small but significant amounts. It is commonly included in the plagioclase crystals or associated with the subprismatic biotite aggregates. Textural evidence indicates that it is older than the magmatic crystallization of the granites considered. The chemical composition of these garnets is very peculiar (table 1, columns 1 to 9; fig. 8), with grossularite content ranging in most cases from 45 to 54 %, almandine 40-45 %, spessartine 3-10 %, and pyrope practically absent. Garnets from xenoliths have identical composition (table 1, cols. 13, 14; fig. 8). These compositional features are very peculiar, and differ significantly from those commonly found in garnets from granitoids and high-grade metapelites (e.g., BELLINI et al., 1979, fig. 8).

The chemistry of the biotite-bearing metagranites is shown in table 2 (cols. 1-8). Fig. 2 (data points 1-8) indicates that the main chemical trends are plausible for common granites, and that all data points may reasonably be related to a single trend, independent of the topographic location of the respective outcrops.

Summarizing and evaluating the bulk of field observations, microscopic features, and chemical data, it is clear that these rocks represent old granites affected by a substantially conservative greenschist facies

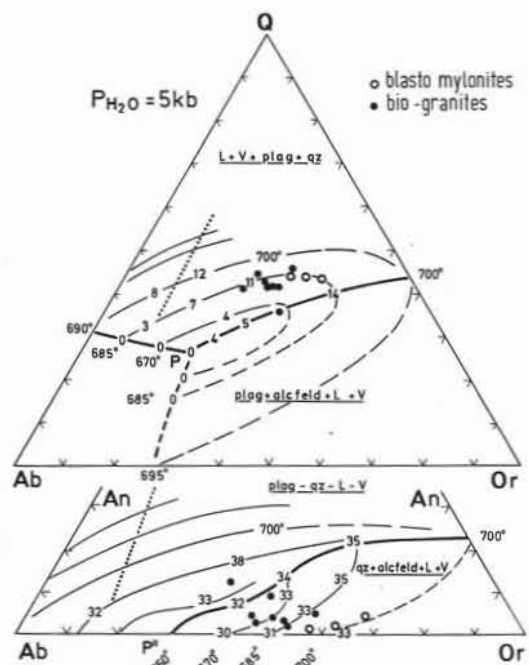


Fig. 3. — Location of the metagranites and blastomylonites in the Qz-Ab-Or-An tetrahedron.

TABLE 2
*Chemical composition of the biotite-bearing metagranites (columns 1 to 8)
 and the blastomylonites (columns 9 to 11)*

	1	2	3	4	5	6	7	8	9	10	11
	8	12	49	50	31	3 FR	30	33	11	52	56
SiO ₂	73,40	74,14	73,49	74,10	72,50	73,41	73,20	74,00	73,00	74,98	73,16
TiO ₂	0,08	0,08	0,19	0,19	0,17	0,32	0,47	0,18	0,55	0,26	0,38
Al ₂ O ₃	14,20	13,43	14,82	13,53	12,90	12,86	13,20	12,60	13,98	13,69	13,66
Fe ₂ O ₃	0,63	0,55	1,53	1,52	1,90	0,37	1,60	0,93	0,55	1,28	1,56
FeO	0,90	1,02	0,10	0,10	1,70	0,96	2,60	0,74	1,45	0,06	0,10
MnO	-	-	0,30	0,02	0,30	-	0,03	0,01	-	0,01	0,01
MgO	0,41	0,37	0,25	0,29	0,42	0,44	0,84	0,39	0,63	0,11	0,49
CaO	0,84	0,80	0,42	0,52	1,40	1,02	1,00	0,61	0,76	0,16	0,32
Na ₂ O	2,31	3,13	2,95	3,01	3,50	3,75	2,90	3,10	1,81	2,27	2,47
K ₂ O	5,16	4,28	4,95	4,95	4,00	4,95	5,00	4,80	6,40	5,65	5,27
P ₂ O ₅	0,29	0,41	0,19	0,16	0,07	0,39	0,06	0,17	0,29	0,19	0,20
H ₂ O+	1,02	0,90	1,07	0,96	1,68	0,23	1,54	0,72	0,93	1,19	2,28
H ₂ O-	0,18	0,50	-	-	-	0,86	-	-	0,06	-	-
Tot.	99,40	99,16	99,99	99,35	100,27	99,56	102,44	98,25	100,41	99,85	99,90
D.I.	26,91	26,308	27,30	27,372	22,937	26,667	23,52	26,89	27,398	29,161	27,343
Ab	21,89	29,50	27,39	27,62	32,76	34,21	27,82	28,75	17,25	20,84	23,59
Or	31,71	25,69	31,13	30,68	22,48	29,12	27,13	28,91	38,83	35,17	32,70
An	2,54	1,43	0,92	1,66	7,17	2,70	5,17	2,09	2,11	0,86	0,31
Qz	43,87	43,38	40,56	40,04	37,59	33,98	39,87	40,24	41,81	43,13	43,60
Ab	22,46	29,93	27,64	28,08	35,29	35,16	29,34	29,37	17,63	21,02	23,67
Or	32,53	26,06	31,42	31,20	24,22	29,92	28,61	29,53	39,67	35,48	32,80
Qz	45,01	44,01	40,93	40,72	40,49	34,92	42,05	41,10	42,71	43,50	43,53
Ab	38,99	52,11	46,08	46,06	52,49	51,81	46,27	48,12	29,65	36,65	41,68
Or	56,49	45,37	52,38	51,17	36,02	44,10	45,12	48,38	66,73	61,84	57,77
An	4,52	2,52	1,55	2,77	11,48	4,09	8,60	3,50	3,62	1,51	0,55

metamorphism. Their history may be classified in two main stages:

(1) magmatic stage, during which a «granitic» mineral assemblages (qz + kf + pl) crystallized from a melt, incorporating inclusions of biotite, white micas, garnet, and white mica pseudomorphs. The lack of Al₂SiO₅ polymorphs among the inclusions is to be stressed. The above-mentioned xenocrystals are to be considered as belonging to the original rock from which the melts formed; however, their chemical composition probably altered as an effect of anatexis and later history;

(2) metamorphic stage, during which the old granites acquired a more or less well-

defined foliation and were affected by complete recrystallization. In particular, magmatic plagioclase altered into albite + sericite + epidote, biotite into Mg-richer biotite (as shown by the ore «exsolution»), and crystal interfaces were modified, also reflecting complicated and changing replacement relationships among the feldspars and feldspars versus micas. It should be emphasized that biotite remains among the stable mineral phases even during the most recent metamorphic evolution of these rocks.

As regards the magmatic stage, in order to estimate the physical conditions which controlled production of the related melts, the chemical data of table 2 were plotted

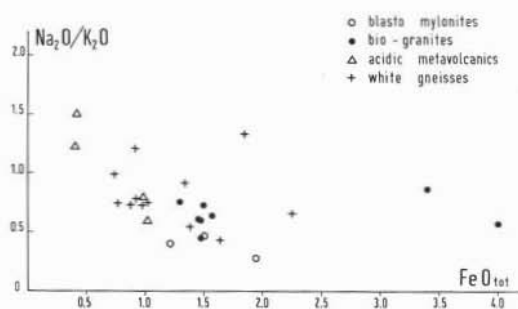


Fig. 4. — FeO_{tot} versus $\text{Na}_2\text{O}/\text{K}_2\text{O}$ displaying compositional analogies between biotite-bearing metagranites and blastomylonites and differences in comparison to acidic metavolcanics and biotite-free gneisses.

into the Qz-Ab-Or-An tetrahedron (WINKLER & BREITBART, 1978) using the mesonorm proposed by MIELKE & WINKLER (1979).

As shown in fig. 3, data points 1-8 cluster within a relatively small volume located slightly below the $L+V+pl+qz$ surface (Q-Ab-Or projection) within the quartz field, relatively close to the cotectic line.

All these rock samples have a surplus of quartz and a deficit of An, both spread over an extremely narrow range. The single values are shown in table 2 and in fig. 3. The values of these surpluses and deficits are lowest if the tetrahedron for $P_{\text{H}_2\text{O}} = 5$ kb is taken as a reference. Therefore, if we assume that these rocks are related to magmas close to ternary minimum melts, it is reasonable to assume the tetrahedron for $P_{\text{H}_2\text{O}} = 5$ kb for a geothermobarometric interpretation. In this case, the conclusion is that these melts formed in the range 670-690° C.

Some acidic gneisses characterized by a more or less intense blastomylonitic texture are to be mentioned here, for their possible original relations with the above metagranitoids.

These rocks typically outcrop in the Rókáñez area, where lineated paragneisses, kyanite-bearing quartzites and leucophyllites also occur. Shearing effects and a micro-augen texture are the most striking features observable in the field.

In thin section, it can be seen that the appearance of the micro-augen texture and

the well-developed foliation are genetically related to a blastomylonitic event. Heteroblastesis is very typical in these rocks, as well as banding produced by alternations of micro-augen-rich and very fine-grained matrix-rich layers.

Most of the augen consist of K-feldspar. They are often fractured, the fragments being sutured mainly by microblastic quartz aggregates. Large white mica flakes, garnet, quartz, albite, biotite, apatite and zircon may be observed as inclusions within the augen.

Plagioclase mainly occurs in the matrix, as fresh granoblasts of albitic composition. Rare albite augen have also been observed, commonly bearing sericite inclusions.

White mica occurs both in large flakes displaying postkinematic deformations (including kink bands), and in minor crystals associated with biotite and quartz in pressure shadows around the augen. Lastly, white mica occurs in the matrix, as small flakes often associated with biotite and ores.

Biotite seems to be a stable mineral phase, and is often in contact with white mica.

The matrix of these rocks consists of quartz, white mica, biotite, albite, and microcline. Quartz commonly forms thin ribbons as an effect of shearing.

Transitions between strongly deformed and less deformed rock types may be observed, the latter displaying a larger grain-size and a less well-defined augen texture.

All these features suggest that the rocks giving rise to these blastomylonites were acidic gneisses having:

- 1) granitic composition;
- 2) significant amounts of biotite and ores;
- 3) relative abundance of white mica in large flakes;
- 4) important amounts of K-feldspar in large crystals.

Based on these considerations, the parent rocks of these blastomylonites are very probably the above-described metagranites (perhaps a fine-grained type), rather than the metavolcanics to be described below. In fact, biotite is lacking or scarce in the latter rocks, their augen mostly consist of plagioclase, and large flakes of white micas are relatively abundant.

TABLE 3
*Chemical composition of acidic metavolcanics (columns 12 to 15)
 and biotite-free white gneisses (columns 16 to 27)*

	12	13	14	15	16	17	18	19	20	21	22	23	24	25	26	27
	13	41	45 A	45 B	1	2	87	90	28	29	4	5	6	14	2 FR	S 600
SiO ₂	74.93	75.02	82.40	82.30	78.08	73.99	74.98	75.40	74.98	75.2	74.20	73.50	71.30	76.39	76.46	73.30
TiO ₂	0.09	0.12	0.07	0.07	0.14	0.10	0.12	0.09	0.12	0.13	0.50	0.01	0.01	0.14	0.25	0.01
Al ₂ O ₃	13.98	13.67	10.04	10.10	12.56	14.84	13.56	13.34	14.10	14.06	11.90	14.50	14.50	12.96	13.21	14.50
Fe ₂ O ₃	0.32	1.01	0.29	0.34	0.77	0.51	0.97	0.68	0.94	1.01	1.80	0.93	0.70	0.77	0.72	1.08
FeO	0.69	0.14	0.13	0.11	0.22	0.92	0.11	0.11	0.13	0.13	0.65	1.00	1.00	0.22	0.11	0.36
MnO	-	0.02	0.01	0.01	0.06	0.02	0.02	0.01	0.01	0.01	-	0.01	0.01	-	-	0.01
MgO	0.25	0.22	0.16	0.13	0.68	0.15	0.19	0.19	0.29	0.26	0.40	0.80	0.02	0.37	0.30	0.02
CaO	0.46	0.47	0.16	0.23	0.45	0.61	0.34	0.33	0.23	0.14	1.12	0.90	1.12	0.45	0.20	1.12
Na ₂ O	3.36	3.06	3.50	3.65	3.55	2.96	3.48	3.91	3.45	3.19	2.72	3.30	2.30	3.21	3.23	3.30
K ₂ O	4.21	5.07	2.61	2.42	2.95	5.56	4.79	4.52	4.18	4.24	4.20	2.50	5.50	4.12	4.39	3.70
P ₂ O ₅	0.28	0.21	0.13	0.10	0.19	0.33	0.20	0.21	0.19	0.19	0.24	0.25	0.15	0.26	0.01	0.20
H ₂ O ⁺	0.89	1.04	0.53	0.49	0.74	0.70	0.88	0.69	1.12	1.17	1.10	n.d.	n.d.	0.87	0.80	n.d.
H ₂ O ⁻	0.02	-	-	-	0.19	0.06	-	-	-	-	-	n.d.	n.d.	0.19	0.03	n.d.
Tot.	100.05	100.03	100.03	99.95	100.58	100.75	99.64	99.48	99.74	99.73	99.33	97.70	96.79	99.95	99.98	97.78
D.I.	27.50	28.34	29.37	29.08	26.93	28.08	27.68	28.41	27.68	27.87	25.31	23.46	26.32	27.85	28.62	25.48
Ab	31.16	27.74	30.57	31.94	32.62	27.17	31.46	34.98	31.57	29.36	25.36	32.54	21.73	29.38	29.33	30.64
Or	25.58	31.23	15.30	14.27	16.74	33.86	29.49	27.54	25.70	26.31	25.06	13.53	34.28	25.00	26.30	22.94
An	0.49	1.02	0.82	0.50	1.07	0.94	0.40	0.28	1.23	0.75	4.38	3.29	5.10	0.57	0.99	4.65
Qz	42.77	40.01	53.31	53.29	49.57	38.03	38.65	37.20	41.49	43.58	45.20	50.64	38.90	45.06	43.37	41.76
Ab	31.32	28.03	30.82	32.10	32.97	27.43	31.58	35.08	31.97	29.59	26.52	33.64	22.89	29.55	29.63	32.14
Or	25.71	31.55	15.43	14.34	16.92	34.18	29.61	27.61	26.02	26.51	26.21	13.99	36.12	25.14	26.57	24.06
Qz	42.98	40.42	53.75	53.56	50.11	38.30	38.81	37.31	42.01	43.91	47.27	52.36	40.99	45.32	43.80	43.80
Ab	54.45	46.24	65.48	68.38	64.68	43.85	51.27	55.71	53.97	52.04	46.27	65.92	35.56	53.47	51.80	52.62
Or	44.70	52.06	32.77	30.54	33.19	54.64	48.07	43.85	43.93	46.62	45.73	27.42	56.10	45.49	46.45	39.99
An	0.86	1.71	1.75	1.08	2.13	1.51	0.66	0.44	2.11	1.34	8.00	6.67	8.35	1.04	1.75	7.99

As shown in fig. 4, this hypothesis is also supported by the chemical data in table 2 (columns and data points 9-11) and figs. 2 and 3. The chemical contents are indeed very close to those of the metagranitoids, and often differ significantly from those of the metarhyolites (table 3, cols. 12-15) and other acidic gneisses (table 3, cols. 16-27) from the Sopron and Fertőrákos areas.

1.2. Acidic metavolcanics and metavolcanoclastics

These rocks are known from the Deákút quarry in the town of Sopron. They are strongly foliated, very often affected by a banded texture, and characterized by the occurrence of numerous small phenocrysts surrounded by a fine-grained matrix. Textural features recalling metamorphic ignimbrites may sometimes be observed in the field.

The changing quantitative ratio between phenocrysts and matrix in these rocks produces important compositional differences

among the various bands, reflecting pre-metamorphic situations related to volcanic activity and interference of subcontemporaneous sedimentary processes. As a consequence, some layers represent original lavas, some volcanoclastics, and some clastic sediments.

The true metavolcanics are characterized by a ratio between phenocrysts and matrix corresponding to porphyritic rhyolites. On the contrary, the metavolcanoclastics commonly bear a surplus of phenocrysts, particularly of quartz in both augen and matrix, while the clastic metasediments display a semi-pelitic composition, although a volcanic contribution may still be recognized in them.

The phenocrysts consist of quartz, K-feldspar, or plagioclase. Polycrystalline augen also occur, consisting of plagioclase + quartz. They are mostly rounded and sometimes have embayed contours. They are commonly fractured, and microblastic quartz aggregates (and sometimes sericite aggregates

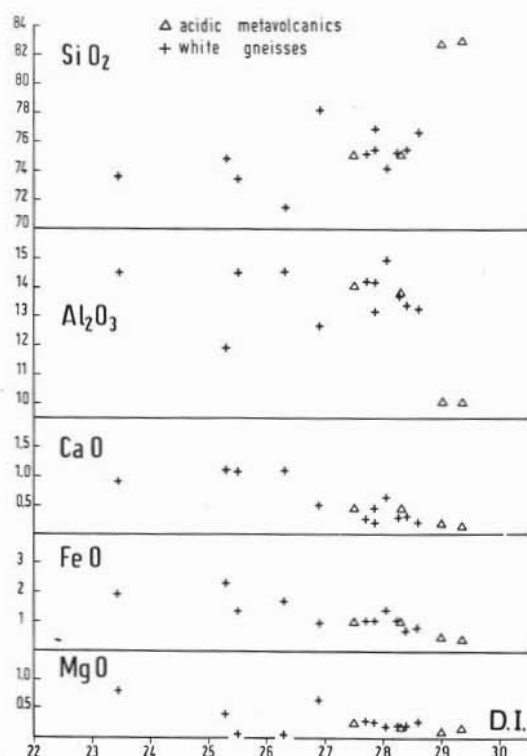


Fig. 5. — Variation diagrams concerning some chemical contents in the acidic metavolcanics and in the biotite-free white gneisses.

in the K-feldspar augen) cement the fractures. Among their inclusions, garnet is worthy of note. Its composition is identical to that of garnets from the biotite-bearing metagranites (table 1, cols. 10-12; fig. 8).

K-feldspar is commonly perthitic and does not display alteration effects. However, chessboard albite sometimes occurs, probably representing original crystals of K-feldspar altered into albite during a late-magmatic stage.

Plagioclase crystals commonly include numerous flakelets of sericite \pm epidote. A relic image of zoning may sometimes be observed.

The fine-grained matrix mainly consists of the above leucocratic minerals. Small biotite flakes sometimes occur, as well as garnet.

The relative abundance of radioactive apatite and other metamictic minerals is worthy of note for its genetic implications

regarding other special rock types occurring in this area (FAZEKAS et al., 1975; LELKES et al., 1983).

Field observations and microscopic features indicate that the original volcanic rock had the following characters: porphyritic texture; quartz, K-feldspar and plagioclase phenocrysts; occurrence of small amounts of garnet and biotite as femic mineral phases.

These rocks were affected by a greenschist facies metamorphism, the main features of which are given by the stability of biotite and albite + epidote.

The chemistry of the metarhyolites is shown in table 3 and figs. 4 and 5 (columns and data points 12-15). These chemical features are not significantly different from those of the metagranites (table 2 and fig. 2).

As regards the location of these rocks within the Qz-Ab-Or-An tetrahedron (fig. 6), two of the four data points (triangles) fall in the same field defined by the biotite-bearing metagranites. They may consequently be interpreted in the same way as the metagranites, and temperatures of 650°-685° C under pressures of 5 Kb may be assumed for them.

The other two data points plot closer to the Ab-Qz side, displaying a significant surplus of Qz. Therefore, they cannot be considered as minimum melts, and a simple geothermometric interpretation is not obvious for them. In our opinion, the most probable explanation is suggested by the above-mentioned frequent occurrences of sedimentary intercalations within these volcanic sequences. Therefore, local mixtures of sedimentary and volcanic materials are to be expected, and quartz enrichment could be an obvious consequence. Indeed, the above-considered rock samples may represent volcano-sedimentary mixtures of this type. This hypothesis is also supported by the Na enrichment of these two rocks, which are the only ones displaying a $\text{Na}_2\text{O}/\text{K}_2\text{O}$ ratio higher than 1 (see also fig. 4).

1.3. White gneisses

These rocks are the most widespread in the Sopron basement, and also occur in the Fertőrákos area. The largest outcrop is the Nándormagaslat quarry near the village of Sopronbánfalva. This is a well-foliated,

medium- to large-grained white gneiss displaying moderate banding and sometimes an augen texture. The changing grain size in different layers enhances the banded texture.

Some augen consist of plagioclase, others of K-feldspar, the latter commonly being larger than the former. The ratio between the two types of augen varies.

Plagioclase includes microliths of sericite \pm epidote, biotite, garnet, apatite, and white mica. It also occurs as small subhedral inclusions in the K-feldspar augen and xenoblasts in the matrix.

K-feldspar is commonly perthitic in both augen and xenoblasts. It includes quartz, white mica, plagioclase, and apatite.

White mica occurs both as large deformed flakes corroded by quartz and plagioclase, and aggregates having a roughly prismatic shape and decussate texture, within which very fine-grained ores are dispersed. These aggregates probably represent pseudomorphs after an Fe-bearing, Al-rich silicate. White mica also occurs as small flakes in the quartz pressure shadows close to the augen.

Biotite is lacking or scarce, but seems to be a stable mineral phase.

Garnet occurs as inclusions within the large plagioclase crystals, or is localized in the two-mica aggregates.

The matrix consists of the minerals mentioned above. Its grain size varies in different layers but as a rule is definitely larger than in the metarhyolites and metavolcanoclastics.

The chemical composition of the white gneisses is shown in table 3 (cols. 16-27) and figs. 4 and 5 (crosses). The relative data points scatter over a considerable area; however, a granite-type composition may be assumed for most of them.

The location of these data points in the Qz-Ab-Or-An tetrahedron is similar to that of the above-considered metagranites and metarhyolites (fig. 6, crosses). However, the existence of samples with a high Qz surplus suggests a stronger affinity with metavolcanoclastic rocks than with metagranites.

This interpretation is strongly supported by textural evidence (banding, augen texture, scarcity of biotite, etc.) and the common association with leucophyllites, which have been interpreted as altered metavolcanics by LELKES et al. (1983). Lastly, it is worth

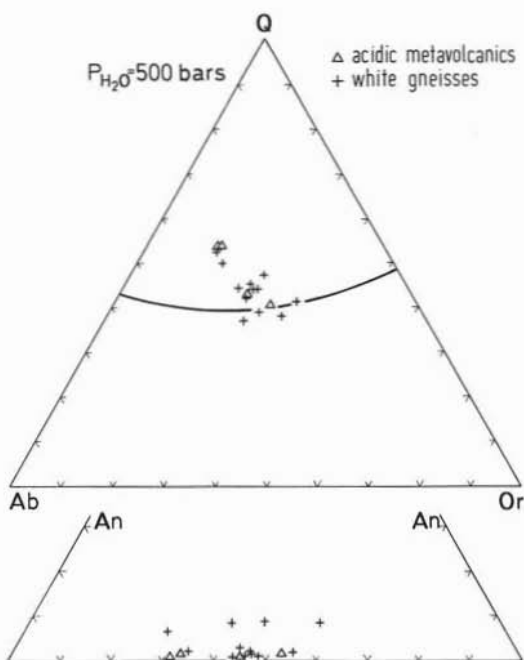


Fig. 6. — Location of the acidic metavolcanics and biotite-free white gneisses in the Qz-Ab-Or-An tetrahedron.

noting that a simple increase in grain size of the matrix in the above metavolcanics and metavolcanoclastic is sufficient to produce rocks identical in texture and mineral composition to the white gneisses.

1.4. Leucosomes

In the Brennerg area near Sopron the outcropping micaschists bear thin layers, lenses and bands up to a few centimeters thick, of acidic composition. The largest lenses of these leucosomes include very thin remnants of former schist layers, subparallel to the boundaries between the leucosomes and the host micaschists.

These micaschists mainly consist of quartz, muscovite, biotite, and plagioclase. The occurrence in them of K-feldspar, andalusite, sillimanite and kyanite (both sometimes included in the andalusite poikiloblasts) is to be pointed out, as well as the stability of muscovite + quartz.

The leucosomes mainly consist of a quartz-feldspar aggregate with panxenomorphic texture, completely lacking in planar anisotropies.

TABLE 4
Microprobe analyses of the garnets from leucosomes and high-grade metapelites
 (columns 1-3; 4-24)

	1 3B ₉₁	2 3 B ₉₂	3 3 B ₉₃	4 30 9 core	5 30 9 interm.	6 30 9 rim	7 12/a rim	8 12/a rim	9 12/a rim	10 12/a interm.	11 12 core	12 12/gr rim
SiO ₂	36,10	36,28	36,49	38,42	38,17	38,28	37,75	37,94	36,43	37,50	37,54	37,72
TiO ₂							0,0	0,0	0,08	0,11	0,13	0,0
Al ₂ O ₃	20,62	20,32	20,27	20,40	20,64	20,95	20,36	20,51	20,43	20,56	20,55	20,01
FeO	34,18	34,16	35,33	33,43	33,53	33,40	35,93	34,62	33,77	32,36	29,59	30,55
MnO	0,15	6,06	5,05	4,82	4,72	4,61	1,74	1,98	2,62	3,03	4,54	4,96
MgO	2,35	2,94	2,48	2,50	2,62	2,55	2,17	1,77	1,91	1,68	1,25	1,60
CaO	0,17	0,19	0,39	0,44	0,33	0,21	2,42	3,02	3,34	4,56	6,34	5,36
Alm	76,3	74,5	77,8	77	77,3	78	80	79	76	73	66	67
Prp	9,2	11,6	9,7	10,3	10,7	10,5	9	7	8	7	5	7
Spa	14	13,4	11,3	11,3	11	11	4	5	6	7	10	11
Grs	0,5	0,4	1,2	1,4	1	0,5	7	9	10	13	19	15

	13 12/gr ₂ rim	14 12/gr ₃ rim	15 12/gr ₄	16 12/gr ₂	17 25330 ₉ core	18 33 ₉₁ rim	19 33 ₉₂ interm	20 33 ₉₃ core	21 33 a core	22 33 b	23 33 c	24 33 d
SiO ₂	39,05	39,05	39,06	38,73	38,07	37,76	35,42	36,50	37,56	37,39	39,95	40,22
TiO ₂	0,0	0,0	0,0	0,0		0,11	0,26	0,15	0,26	0,0	0,0	0,0
Al ₂ O ₃	20,94	20,99	21,37	21,39	20,77	20,14	19,36	19,64	20,20	20,42	22,00	21,91
FeO	31,84	29,83	33,85	31,78	32,98	38,15	35,29	31,13	34,01	37,62	37,68	35,55
MnO	2,0	2,95	1,48	2,73	5,11	1,56	4,27	0,26	4,40	2,06	1,77	2,51
MgO	1,79	1,34	2,19	1,80	2,79	1,63	1,04	0,45	1,08	1,67	1,76	1,69
CaO	4,92	6,60	2,46	3,98	0,28	0,64	2,14	4,57	2,47	0,76	0,98	2,05
Alm	73	68	80	74	75,8	87	80	70	78	86	86	81
Prp	7	6	9	8	11,4	4	4	2	5	7	7	7
Sps	5	7	3	6	11,9	7	10	15	10	5	4	6
Grs	15	19	8	12	0,9	2	6	13	7	2	3	6

Quartz crystals are xenomorph, sometimes surrounded by sillimanite needles and often affected by post-crystalline deformations.

K-feldspar occurs as large, perthitic, anhedral crystals, largely altered into sericite. Small white mica flakes appear within the sericite pseudomorphs after plagioclase.

Small garnet idioblasts are often included in the plagioclase crystals. Their chemical composition is shown in table 4 (cols. 1-3) and fig. 8, displaying strong compositional similarities with the garnets from high-grade metapelites.

Biotite displays two types of occurrence. Reddish-brown (to yellow) biotite flakes are

included in quartz crystals or occur in the matrix associated with white mica and/or sillimanite. Light green (to yellow) biotite flakes only occur within the characteristic pseudomorphs (after cordierite?), described below.

Sillimanite needles are associated in fibrolitic aggregates with white mica and/or reddish-brown biotite.

Some fine-grained aggregates of sericite + chlorite + greenish biotite + disseminated ore minerals typically occur in these leucosomes. They are sometimes sub-euhedral but mostly have irregular shapes. They sometimes include small garnet crystals. These aggregates certainly formed by replacement

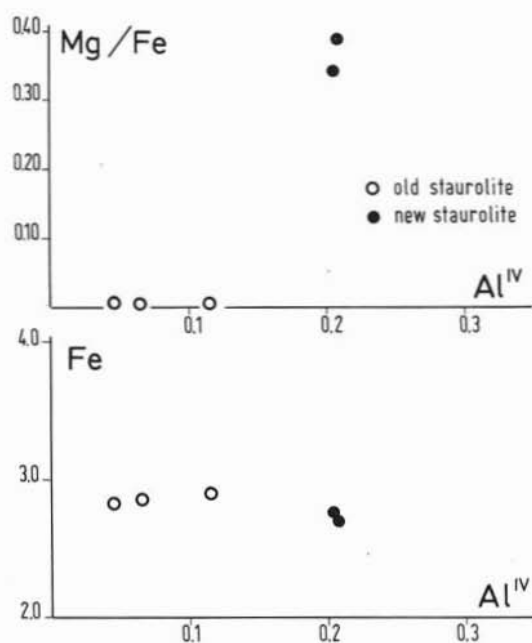


Fig. 7. — Main compositional differences between the old and the young staurolite crystals.

after an old, now completely obliterated, mineral phase. Considering their shape and the chemical composition of the replacing phases, these aggregates may represent pseudomorphs after cordierite.

The pre-metamorphic mineral assemblage in the leucosomes was probably quartz + K-feldspar + plagioclase + biotite + cordierite? + sillimanite. The main mineral alterations indicate that these rocks only underwent a low-grade metamorphism without important penetrative deformations.

2. Metapelites and related schists

Metapelites and metasemipelites are widespread in the Sopron basement, displaying complex metamorphic development and various metamorphic grade, which ranges from the lower sillimanite zone (Brennberg-banya) to the chloritoid + almandine zone (upper greenschist facies: e.g., at Vöröshid). Phyllites of probably lower metamorphic grade (chlorite + muscovite) are relatively common and have also been found in deep drillings (e.g., borehole Sopron-8, in which

TABLE 5
Semiquantitative composition of biotites from leucosomes (columns 1-2) and metapelites (col. 3-6)

	1	2	3	4	5	6
	3 B _{D2}	3 B _{B3}	12 b ₁	33 b ₁	33 b ₂	33 b _{2A}
SiO ₂	37.2	37.1	40.7	40.00	40.1	41.6
TiO ₂	0.9	1.2	1.3	1.7	1.3	1.6
Al ₂ O ₃	21.1	20.5	20.0	20.3	19.4	20.8
FeO	17.6	17.6	17.5	20.4	20.2	19.7
MnO	0.2	0.1				
MgO	11.9	11.3	12.3	10.3	9.2	10.6
K ₂ O	7.8	7.6	6.1	7.8	7.7	7.7
Si	5,920	5,975	6,159	5,943	6,155	6,078
Al ^{IV}	2,080	2,025	1,841	2,057	1,845	1,922
Al ^{VI}	1,881	1,878	1,724	1,494	1,66	1,657
Ti	0,110	0,147	0,154	0,196	0,156	0,175
Fe	2,346	2,381	2,213	2,543	2,585	2,412
Mn	0,029	0,022				
Mg	2,831	2,714	2,776	2,284	2,097	2,316
K	1,584	1,568	1,188	1,481	1,50	1,439

TABLE 6
Microprobe analyses of staurolite from metapelites (col. 4-5: old; col. 1-3: young)

	1	2	3	4	5
	25330 St ₁	30 St ₂	30 St ₃	17 St ₁	17 St ₂
SiO ₂	26.44	28.04	28.19	28.03	28.42
TiO ₂	0.12	0.36	0.02	0.46	0.40
Al ₂ O ₃	54.67	54.35	54.53	54.14	54.60
FeO	12.17	12.39	12.11	11.87	11.77
MnO	0.56	0.33	0.56	0.19	0.20
MgO	-	-	-	2.29	2.59
CaO	0.11	0.09	-	n.d.	n.d.
Na ₂ O	-	0.44	-	-	-
Tot.	96.07	96.00	95.51	96.98	97.99
Si	7,9545	7,8828	7,9361	7,7943	7,7923
Al ^{IV}	0,0455	0,1172	0,0639	0,2057	0,2077
Al ^{VI}	17,9734	17,8868	18,0260	17,5341	17,4264
Ti	0,1008	0,0759	0,0091	0,0484	0,0823
Fe	2,8458	2,9126	2,8508	2,7590	2,6965
Mn	0,1327	0,0777	0,1336	0,0451	0,0461
Ca	0,0336	0,0270	-	-	-
Mg	-	-	-	0,9486	1,0569
Na	-	0,0295	-	-	-
	21,0863	21,009	21,0195	21,33	21,308

these rocks were found from 500 m to the bottom of the hole, i.e., to 649 m, below muscovite gneisses).

We will only consider here the petrographic features of the Al-rich metapelites

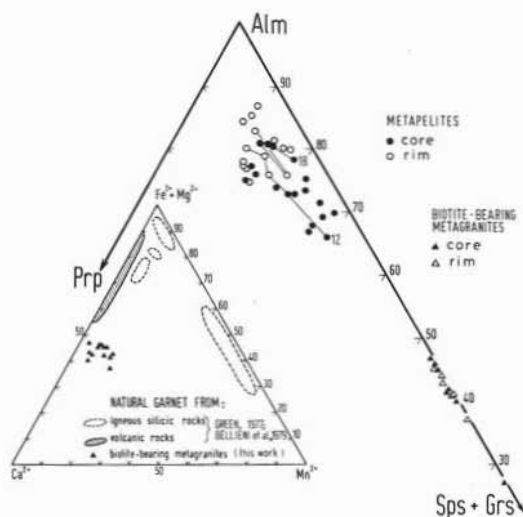


Fig. 8. — Composition of the garnets from: biotite-bearing metagranites, their xenoliths and acidic metavolcanics ($\blacktriangle\triangle$); metapelites and leucosomes ($\bullet\circ$).

in the amphibolite facies, because they display a long metamorphic history with plurifacial character. In these rocks, indeed, the occurrence and mutual relationships among the Al_2SiO_5 polymorphs and other Al-rich mineral phases are complex. A powerful time-marker for unravelling this complex metamorphic history is represented by the very common andalusite porphyroblasts.

Sillimanite occurs as medium to small crystals, generally associated in large aggregates fringed by fibrolite. Biotite is generally intimately associated with sillimanite, and textural evidence indicates that this sillimanite crystallization took place at a very early stage of the metamorphic development of these rocks: sillimanite crystals and aggregates are indeed commonly included within andalusite poikiloblasts.

The occurrence of a younger sillimanite generation cannot be excluded, as suggested by some sillimanite crystals which are not included in the andalusite poikiloblasts, and are sometimes nucleated at their boundaries.

Kyanite occurs in two different textural situations, believed to be related to two different crystallization times. The older kyanite crystals are systematically included within the andalusite poikiloblasts, where

they form both relatively large individuals and radial aggregates of small acicular crystals. The younger kyanite crystals are small idioblasts, systematically located within sericite aggregates, where they are often associated with euhedral chloritoid crystals.

Staurolite also occurs in two differently aged textural situations. Small staurolite crystals included within the andalusite poikiloblasts and irregularly shaped staurolite fragments located within the above sericite pseudomorphs are the relics of the old staurolite generation. The different fragments occurring in the same sericite aggregate sometimes have identical optical orientation, demonstrating that they represent dismembered parts of a formerly single larger crystal. The younger staurolite crystals are small idioblasts located within the sericite pseudomorphs. They have the identical textural features and microscopic aspect of a similar staurolite occurrence within the Austridic metapelites outcropping further to the west in Pusteria (CONTINI & SASSI, 1980, figs. 8 and 9).

Microprobe analyses of the young and old staurolite crystals are shown in table 6 (cols. 1-3 and 4-5 respectively). The main compositional differences between the young (dots) and old (crosses) staurolite crystals are shown in fig. 7.

The above-mentioned sericite pseudomorphs are often prismatic or subprismatic in shape. The occurrence in them of both staurolite relics and newly formed kyanite + chloritoid idioblasts suggests that these sericite aggregates are pseudomorphs after staurolite porphyroblasts. Flattening effects

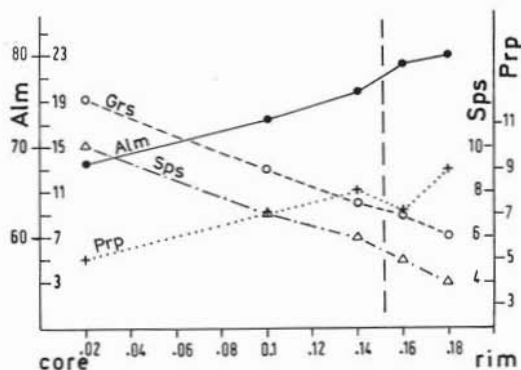


Fig. 9. — Zoning of a garnet crystal from high-grade metapelites (BRENNBERG) (sample 12).

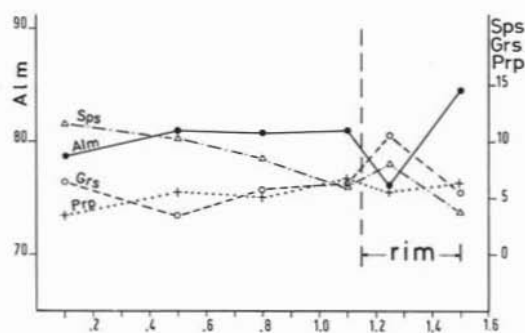


Fig. 10. — Zoning of a garnet crystal from low-grade metapelite (sample 18A).

are common around the sericite pseudomorphs, but the sericite aggregates do not display the expected deformation: this indicates that the flattening phase is older than the sericitization of the former porphyroblasts.

Chloritoid occurs in variously sized crystals. The smaller ones are euhedral, often twinned, systematically undeformed, and located within the sericite pseudomorphs. The larger ones are strongly deformed and perhaps related to an older crystallization phase. The later crystals only occur in the low-grade rocks (upper greenschist facies). Microprobe analyses of six chloritoid idioblasts associated with kyanite within sericite pseudomorphs are given in table 7.

Garnet certainly crystallized during two

TABLE 7
Microprobe analyses of chloritoid from metapelites

	1 12 c ₁	2 12 c ₂	3 12 c ₃	4 33 c ₁	5 33 c ₂	6 33 c ₃
SiO ₂	28,31	28,74	28,75	28,30	28,34	29,92
TiO ₂						
Al ₂ O ₃	43,22	42,97	42,76	43,17	42,99	42,56
FeO	25,23	25,09	24,97	26,09	26,38	25,38
MnO	0,22	-	0,25	0,29	0,20	0,04
MgO	2,98	3,16	3,16	1,96	2,03	1,66
CaO	0,03	-	0,04	0,10	0,02	-
Si	2,14	2,17	2,17	2,15	2,15	2,26
Al	3,85	3,82	3,80	3,86	3,85	3,79
Fe	1,59	1,58	1,58	1,66	1,67	1,60
Mn	0,01	-	0,01	0,02	0,01	-
Mg	0,33	0,36	0,36	0,22	0,23	0,19

different metamorphic events or phases. Garnet xenoblasts enclosed within larger garnet crystals having a different colour are to be referred to the older event, together with large euhedral crystals and glomeroblasts (up to 5 mm), which are often deformed and dismembered into several fragments. The new garnet generation, in addition to rims around older garnets, is represented by small euhedral crystals often associated with or including small chloritoid idioblasts.

Table 4 (cols. 4-24) shows microprobe analyses of garnets from high-grade metapelites. Table 8 refers to garnets from the upper greenschist facies. These chemical data give the following information:

TABLE 8
Microprobe analyses of garnets from low-grade metapelites

	1 18A ₁	2 18A ₂	3 18A ₃	4 18A ₄	5 18A ₅	6 18A ₆	7 18C ₁	8 18C ₂	9 18C ₃	10 18C ₄	11 18C ₅	12 18C ₆	13 18C ₇	14 18C ₈
	Core			Rim I			Core	Core	Core	Core	Core	Rim I	Rim E	Rim E
Si O ₂	37,58	37,55	38,12	37,59	37,49	37,33	38,13	37,94	37,90	38,16	38,22	38,12	37,98	37,96
Al ₂ O ₃	20,00	20,29	20,07	21,29	20,14	20,73	20,40	20,11	20,22	20,00	20,47	20,16	20,33	20,47
Fe O	34,48	35,37	35,60	35,73	33,85	36,95	29,98	32,38	31,33	34,56	34,99	32,55	36,81	35,83
Mn O	5,01	4,39	3,66	2,62	3,49	1,66	7,14	4,67	5,51	3,81	3,12	4,62	0,87	0,88
Mg O	0,87	1,39	1,24	1,69	1,39	1,51	0,94	1,01	0,85	0,78	1,06	0,78	1,86	1,26
Ca O	2,17	1,02	2,01	2,08	3,64	1,83	3,40	3,69	4,19	2,67	2,15	3,27	2,01	2,28
Alm	78,6	81	80,8	81	76	84,6	69,3	73,8	71,5	80	81,8	75,6	84,5	85,5
Prp	3,5	5,6	5	6,8	5,5	6,2	4	4,1	3,4	3	4,4	3,3	7,6	5,4
Sps	11,6	10,2	8,4	6	8	3,8	16,7	11,2	12,7	9	7,4	11,3	2	2,1
Grs	6,3	3,2	5,8	6,2	10,5	5,4	10	10,9	12,4	8	6,4	9,8	5,9	7

1) the data points of the analysed garnet crystals fall close to the almandine corner and along the spessartine + grossularite side of the (alm)-(spes+gross)-py triangle (fig. 8). They occupy the compositional field usually defined by garnets from amphibolite facies (almandine content higher than approx. 80%: e.g., GOMEZ-PUGNAIRE & SASSI, 1983, fig. 3) and upper greenschist facies (almandine content in the range 70-80%: e.g., CARDIN et al., 1984);

2) all the analysed crystals are zoned, although the difference in chemical contents between cores and rims is slight in some cases;

3) zoning commonly displays the usual bell-shaped pattern, with an increase in almandine and pyrope contents towards the rims, coupled with a decrease in spessartine and grossularite contents (fig. 9);

4) if the main compositional range of the garnets under increasing temperature is represented by increasing almandine contents, the zoning of the analysed garnet crystals may be interpreted as due to increasing temperatures;

5) some garnet crystals display a sharp compositional change at the passage from core to rim. This discontinuity may be related to a two-event crystallization: the rim began to crystallize under completely new physical conditions which later evolved due to increasing temperatures, as suggested by the increase in almandine and pyrope contents and decrease in spessartine and grossularite contents (fig. 10).

Biotite occurs in numerous textural situations. Biotite flakes intimately associated with muscovite including andalusite are to be mentioned, as well as those in which sillimanite nucleated. Semiquantitative microprobe data concerning biotite flakes in contact with garnet are given in table 5, cols. 3-6.

The white mica occurrences include large post-kinematic flakes crystallizing around andalusite or sillimanite, sometimes associated with biotite.

Lastly, the occurrence of some special fine-grained aggregates is to be mentioned. These consist of sericite + chlorite + disseminated

Fe oxides, and often include sillimanite. They may be considered as possible pseudomorphs after cordierite.

As the above description shows, mineral phases which are mutually incompatible occur in the same rocks and in the same thin sections. All the observed microtextural situations and the constraints given by the possible mineral compatibilities point to the polymetamorphic development of these rocks.

3. Amphibolites

Amphibolitic rocks are rare in the Sopron basement, in which they have only been found in deep drillings, while they prevail in the Fertőrákos basement.

3.1. Amphibolites from Sopron area

In the Sopron basement, amphibolitic rocks occur as relatively thin intercalations (1-9 meters) within micaschists or associated with muscovite gneisses. They are banded amphibolites, in which fine-grained amphibole-rich bands alternate with plagioclase-rich bands.

These amphibolites have a micro-augen lined microtexture and consist of the following minerals: amphibole, epidote, clino-

TABLE 9
Microprobe analyses of amphiboles
from the Sopron amphibolites

	29 A ₁ rim	29 A ₂ int.	29 A ₃ core	32 A ₁ core	32 A ₂ core	32 A ₃ core	32 A ₄ rim
SiO ₂	58,37	53,12	49,24	48,40	48,00	46,24	53,11
TiO ₂	0,00	0,12	0,29	0,35	0,40	0,49	0,54
Al ₂ O ₃	1,32	5,94	10,62	10,97	11,73	14,03	4,89
FeO	12,16	11,78	12,64	13,33	12,95	13,58	12,17
MgO	19,31	16,83	14,13	13,69	13,56	12,28	16,92
MnO	0,20	0,19	0,17	0,42	0,17	0,35	0,14
CaO	12,32	11,98	11,79	11,66	11,66	11,19	11,71
Na ₂ O	0,00	0,00	0,91	1,04	1,26	1,52	0,39
K ₂ O	0,05	0,05	0,20	0,15	0,28	0,33	0,13
Si	7,8004	7,3679	6,9428	6,8493	6,7971	6,5789	7,4217
Al ^{IV}	0,1996	0,6321	1,0572	1,1507	1,2029	1,4211	0,5783
Al ^{VI}	0,0084	0,3393	0,7081	0,6795	0,7554	0,9322	0,2273
Fe ^{III}	0,1827	0,2589	0,0029	0,0842	0,0000	0,0000	0,1087
Fe ^{II}	1,1764	1,1076	1,4876	1,4934	1,5337	1,6159	1,3136
Mg	3,8458	3,4790	2,9692	2,8873	2,8617	2,6038	3,5238
Mn	0,0236	0,0223	0,0203	0,0503	0,0204	0,0432	0,0166
Ti	0,0000	0,0125	0,0308	0,0372	0,0426	0,0524	0,0568
Ca	1,7641	1,7805	1,7812	1,7681	1,7692	1,7059	1,7534
Na	0,0000	0,0000	0,2488	0,2854	0,3289	0,3718	0,1057
K	0,0085	0,0088	0,0360	0,0271	0,0506	0,0599	0,1288
Actin.		Ho-act	Mg-Ho	Mg-Ho	Mg-Ho	Mg-Ho	Ho-act.

TABLE 10

Chemical composition of amphibolites from Fertörakos (col. 1-7) and Sopron areas (col. 8-9)

	1	2	3	4	5	6	7	8	9
	SS	ST	PH 1	FR 2	FR 13	FR 21	FR 22	FR 23	FR 37
SiO ₂	55,38	47,90	47,20	49,58	52,20	50,50	52,20	48,60	47,60
TiO ₂	1,19	1,50	1,66	1,63	1,70	1,80	1,70	1,70	2,00
Al ₂ O ₃	17,50	16,20	14,39	14,08	12,70	15,70	12,50	12,70	14,60
Fe ₂ O ₃	2,73	2,10	3,44	3,03	1,20	3,80	3,20	3,30	3,00
FeO	4,14	7,30	10,07	8,77	8,30	8,30	7,80	8,40	9,00
MnO	n.d.	0,007	n.d.	n.d.	0,13	0,33	0,22	0,26	0,06
MgO	4,88	7,40	6,45	7,29	4,80	5,20	5,90	4,40	5,60
CaO	6,95	9,20	10,21	10,12	6,30	7,60	9,20	9,20	10,90
Na ₂ O	1,65	1,90	2,74	2,97	3,10	3,40	3,30	3,60	2,60
K ₂ O	1,81	4,80	0,46	0,65	0,87	1,60	0,10	1,30	0,50
F ₂ O ₃	0,16	0,19	0,39	0,14	0,21	0,74	1,30	1,20	0,18
L.o.i.	2,95	1,40	1,28	0,74	6,30	3,40	4,40	4,50	2,00
Tot.	99,34	99,96	98,62	99,00	97,81	102,57	101,62	99,16	98,04

zoisite, albite, chlorite, and titanite. Rutile, apatite, biotite and quartz may appear as accessory components. Sericite occurs as a secondary mineral after plagioclase.

Amphibole appears in two different textural situations, to which two different compositions correspond: (1) deformed, large nematoblasts of Mg-hornblende (table 9, cols. 3-6), partially altered into chlorite along the cleavage planes, and sometimes including biotite; (2) actinolitic hornblende to actinolite (table 9, cols. 1, 2, 7), which either defines the lined microtexture of these rocks with their small subhedral crystals or make up the rims of the large Mg-hornblende nematoblasts.

Albite makes up anhedral crystals which include numerous grains of clinozoisite and sericite, displaying the features of the so-called « gefüllte » plagioclases. These albite crystals clearly formed by low-grade metamorphic alteration of former An-rich plagioclases.

In addition to the flakes included in the Mg-hornblende porphyroblasts, chlorite occurs in pressure shadows around these porphyroblasts, associated with quartz and white mica.

Biotite only forms small intergranular flakes.

Titanite occurs either as euhedral isolated crystals, aggregates and trails of idioblasts, or rims round rutile.

The pre-metamorphic mineral association which may reasonably be assumed is horn-

blende + plagioclase (disregarding accessory components).

The main metamorphic reactions altered the former plagioclase into albite + epidote, and the former hornblende into actinolite. These alterations imply physical conditions corresponding to the greenschist facies.

Table 10 (cols. 1-2) shows the main chemical features of the Sopron amphibolites. These features will be discussed below, together with those of the Fertörakos amphibolites, as regards their genetic implications.

3.2. Amphibolites from Fertörakos area

Amphibolitic rocks are widespread in the Fertörakos area, making up both the deeper part of the rock columns drilled by boreholes, and numerous conformable intercalations within the prevailing gneisses and metapelites.

These amphibolites are massive, of various grain size, and often banded due to repeated changes of the plagioclase/amphibole ratio. Bands rich in quartz and biotite were sometimes observed.

The most abundant minerals in these amphibolites are amphibole, epidote, clinozoisite, albite, chlorite, and titanite. Sericite, biotite and garnet, when they occur, are accessory components, but may be abundant in some levels.

The amphibole is a green hornblende displaying the same optical features as the analysed Mg-hornblendes from the Sopron amphibolites. It is intimately associated with chlorite ± epidote, in which hornblende is altered locally.

Albite occurs in anhedral crystals which include numerous small grains of clinozoisite and sericite. These crystals are clearly the products of the low-grade metamorphic alteration of An-rich plagioclases.

The original main mineral composition of these rocks was amphibole + plagioclase ± biotite. The protoliths were affected by greenschist facies metamorphism.

Table 10 (cols. 3-9) shows the main chemical features of these amphibolites. These chemical data supply information on the magmatic or sedimentary nature of the protoliths. Figs. 11, 12, 13 and 14 show the diagrams of NIGGLI (1920), LEAKE (1964) and KUNO (1968): the location of

the data points in them support a magmatic origin, as do other diagrams (e.g., TiO-F; SURIYA, 1971) which are not shown in the present paper for space-saving reasons.

As a consequence of the above observations, we are inclined to consider as ortho-amphibolites the Fertőrákos amphibolites and, with a lower degree of certainty (due to the very low number of chemical data) the Sopron amphibolites too.

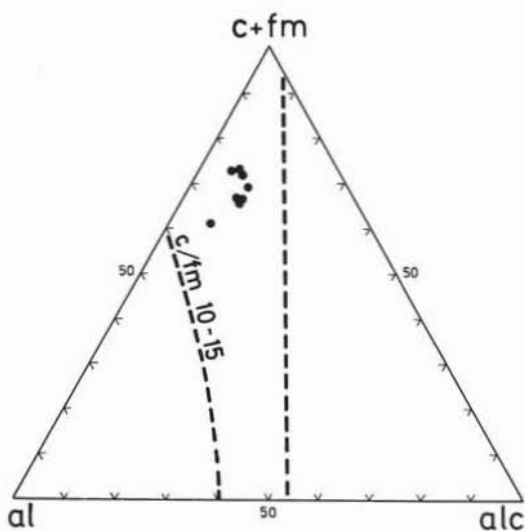


Fig. 11. — $(c + fm)$ -al-alk diagram of the amphibolites of the Sopron and Fertőrákos area.

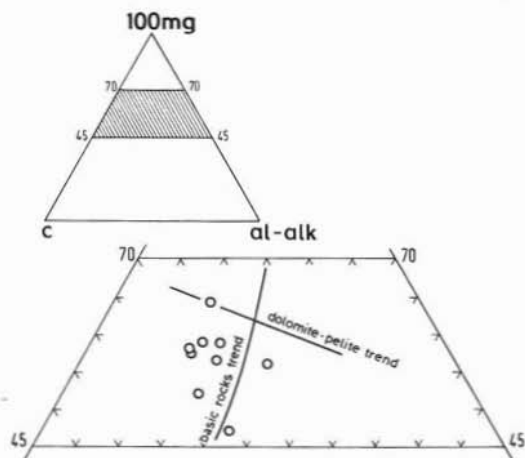


Fig. 12. — 100 mg-c(al-alk) diagram of the amphibolites of the Sopron and Fertőrákos area.

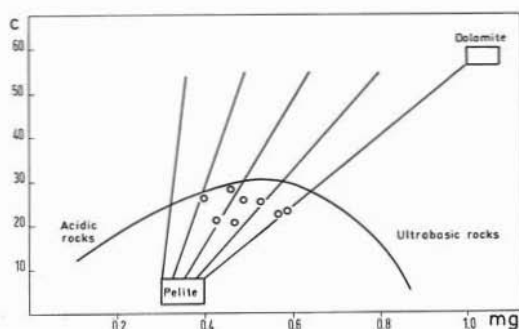


Fig. 13. — c - mg diagram of the amphibolites of the Sopron and Fertőrákos area.

4. Conclusions

The data shown in the preceding sections are used here in order to present models of the metamorphic development of the Sopron basement and its regional evolution.

A. *Metamorphic development.* Textural features and mineral equilibria indicate that these rocks are polymetamorphic, as many authors (KISHÁZI, 1977 and references quoted in it) have recognized.

All data are consistent with a three-stage development, and present knowledge on the evolution of the Austrides in the Eastern Alps (SASSI et al., 1975 publ. 1978; BÖGEL et al., 1978; SASSI & SCHMIDT, 1982) suggests that the oldest stage corresponds to the « Caledonian » event, the middle one to the Hercynian, and the youngest to the Alpine cycle.

The « Caledonian » metamorphism is responsible for the crystallization of the oldest minerals commonly recognizable in the Sopron metapelites by means of textural analysis. They are staurolite, kyanite and garnet porphyroblasts, to which fibrolitic sillimanite must be added in some cases. The « Caledonian » mineral assemblages therefore indicate physical conditions corresponding to an almandine-amphibolite facies related to an « intermediate » metamorphic thermic gradient, the value of which was less than $34^{\circ}\text{C}/\text{km}$ (SASSI et al., 1979). This estimation is consistent with that proposed by SASSI & ZIRPOLI (1979) for other parts of the Eastern Alps.

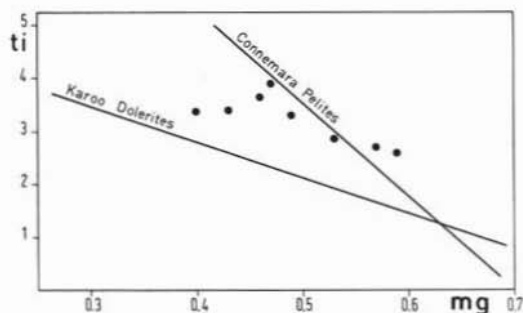


Fig. 14. — *ti-mg* diagram of the amphibolites of the Sopron and Fertőrákos area.

The effects of the *Hercynian metamorphism* are different in different outcrops. The highest Hercynian metamorphic grade was detected in a small quarry in the Brennbergbánya area, where andalusite + sillimanite formed abundantly, together with probable cordierite and perhaps garnet. Leucosomes of granitic composition are also common.

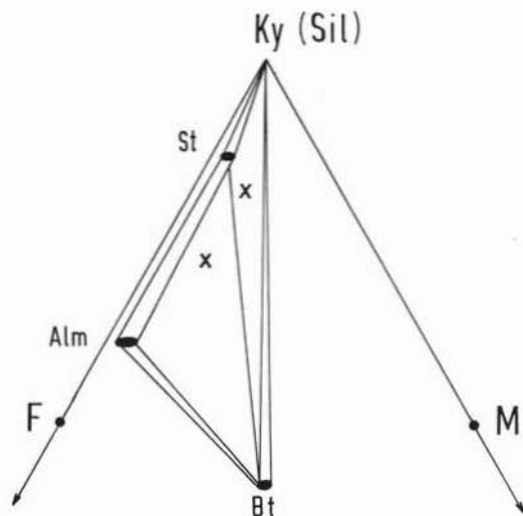


Fig. 15. — Mineral compatibilities of the Caledonian stage.

Elsewhere, the Hercynian metamorphism had a typical retrograde effect, with alteration of staurolite and kyanite porphyroblasts into aggregates of sericite ± chlorite ± ores. Some large chloritoid crystals, local alteration of staurolite into chloritoid, and the local chloritization of garnet porphyroblasts may also tentatively be referred to this event.

Thermally consistent effects occur in the

biotite-bearing metagranites, acidic metavolcanics and metavolcanoclastics, and in the white gneisses. The age of these effects, however, is not well established: it could be Hercynian or Alpine (see discussion below).

From the above data, the Hercynian metamorphism is to be related to a large thermic range (mainly greenschist facies and local amphibolite facies) in the context of a metamorphic thermal gradient higher than 34° C/km (SASSI et al., 1979). The value assigned to the Hercynian thermal gradient by BÖGEL et al. (1979) is compatible with these results.

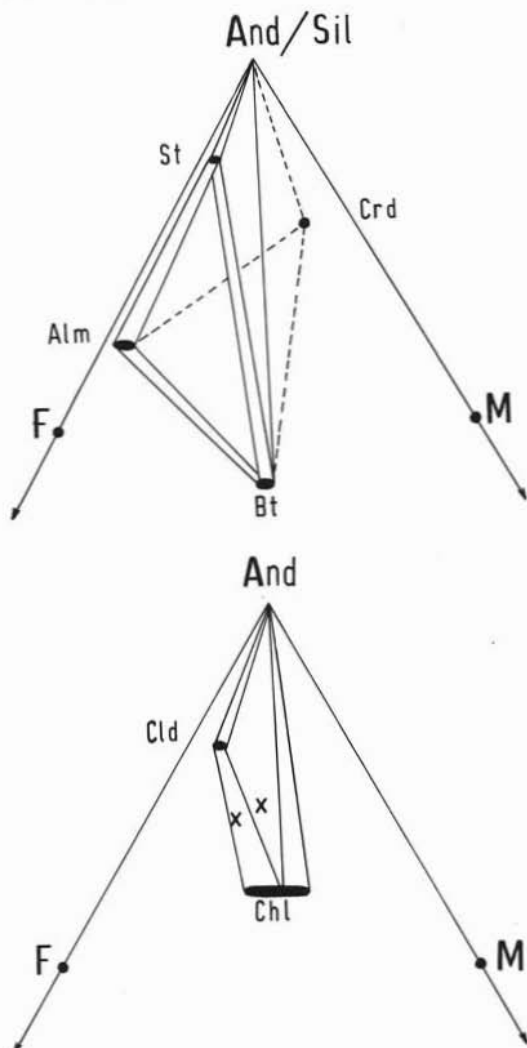


Fig. 16. — Mineral compatibilities of the Hercynian stage.

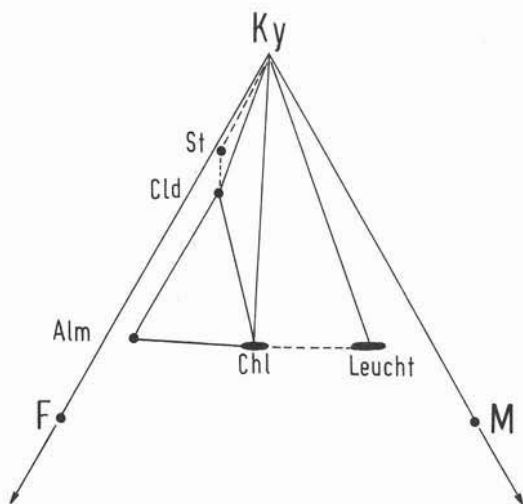


Fig. 17. — Mineral compatibilities of the Alpine stage.

The main effects of the *Alpine metamorphism* are easily recognizable. The most typical are: small chloritoid and kyanite idioblasts usually located within sericite patches, rare staurolite idioblasts located in the same patches, and perhaps small garnet idioblasts. The leuchtenbergite-bearing mineral assemblages reported by LELKES et al. (1983) should also be referred to this event. The prevailing thermal conditions to be related to Alpine metamorphic reworking on the basis of the significant mineral crystallizations are those of the greenschist facies; only locally were temperatures allowing the stability of staurolite reached. The Alpine thermal gradient was lower than $34^{\circ}\text{C}/\text{km}$ (SASSI et al., 1979), as shown by the stability of kyanite. This estimation is consistent with the values of Alpine metamorphic thermal gradients quoted in the literature on the Eastern Alps (SASSI et al., 1980 b).

In the above pictures of the three metamorphic stages detected in the Sopron basement, only the most petrologically significant and clear mineral crystallizations have been mentioned. It is obvious, however, that other minerals crystallized in each stage, specifically those which would be expected in the given physical conditions. Most of the microscopic data are consistent with this statement.

B. Regional evolution. The data shown in the present paper represent a contribution to further knowledge on the regional evolution of the Sopron area. However, they are not sufficient for formulating a single model of the succession of geological processes. In fact, although the chronological constraints supplied by the geo-petrologic situations indicate at least two main models, radiometric geochronologic data pointing to the right solution are not available.

Consequently, two alternative models will be presented here and the reliability of each of them discussed. Amphibolites and the related magmatic activity will be disregarded, due to the scarce exposure of these rocks in the field. For the same reason, the Fertörakos area will not be inserted in the following models, which refer to the Sopron area only.

Model A. According to this model, the following succession of events is recorded in the Sopron area:

1. Pre-Hercynian metamorphism, which developed under amphibolite facies conditions related to a metamorphic thermal gradient lower than $34^{\circ}\text{C}/\text{km}$ (assumed age: Lower Ordovician).

2a. Acidic magmatic activity, which developed both under plutonic (above-described biotite-bearing granites) and volcanic (above-described rhyolites and related rocks) conditions (assumed age: Upper Ordovician and/or middle part of the Ordovician).

b. Alteration of the above volcanics and volcanoclastics, producing materials from which leucophyllites and related rocks derived (LELKES et al., 1983) (assumed age: hydrothermal stage of above volcanism).

3. Hercynian metamorphism, which developed under a large range of temperatures related to a metamorphic thermal gradient higher than $34^{\circ}\text{C}/\text{km}$ (assumed age: Lower Carboniferous).

4. Alpine metamorphism, which developed mainly under greenschist facies conditions and, locally, lower amphibolite facies conditions, both related to a thermal gradient lower than $34^{\circ}\text{C}/\text{km}$.

In the ambit of this model, either the materials mentioned in point 2*b* escaped Hercynian metamorphism (they consequently represent Alpine monometamorphic rocks), or they underwent a very low-grade Hercynian metamorphism and the leucht+ky mineral assemblage is Alpine.

Model B. This differs from Model A due to the different assumed age of the acidic magmatic activity, which may indeed be younger than Model A indicates, because there is no conclusive proof that the meta-granites and metavolcanoclastics are poly-metamorphic. Therefore, the succession of events may have been as follows:

1. « Caledonian » metamorphism, as described under Model A, point 1.

2. Hercynian metamorphism, as described under Model A, point 3.

3*a.* Acidic magmatic activity, which developed under plutonic and volcanic conditions, as described under Model A, point 2 (assumed age: Upper Carboniferous/Lower Permian).

b. Alteration of the above volcanics etc., as described under Model A, point 2*b*.

4. Alpine metamorphism, as described under Model A, point 4, adding the leuchtenbergite-bearing mineral assemblages to the certainly Alpine metamorphic crystallization.

Discussion. Definite data indicating conclusive preference in favour of one of the two proposed models are not available. Furthermore, a third model based on the possibility that an Upper Ordovician and an Upper Carboniferous volcanism both operated cannot be excluded completely.

This third model is believed by us to be the least probable, mainly due to the fact that it is highly improbable that identical peculiar processes (such as the very particular alteration of the volcanics under points 2*b*/Model A and 3*a*/Model B) operated twice in the same area, 150-200 millions years one after the other.

As regards the other two models, Model A is strictly consistent with present knowledge on the Austrides of the Eastern Alps (as summarized, for example, in SASSI et al., 1980, and SASSI & SCHMIDT, 1982). On the contrary, Model B is characterized by elements which are completely new for the Austrides in the Eastern Alps, specifically the large amount of Permian granitoids and acidic volcanics.

This fact is not sufficient to assign lower reliability to Model B, but it is sufficient to admit the need for a conclusive demonstration before significantly modifying the evolutionary picture presently available for the Eastern Alps. Such a demonstration can only be supplied by radiometric geochronology, because field data potentially providing clearcut solutions are not expected in the Sopron area, due to poor exposure and the many tectonic complications.

Acknowledgements. — This research was carried out in the framework of IGCP Project No. 5.

The authors acknowledge the support received from P. KISHAZI, L. KOSA, V. FAZEKAS and J. IVANCSICS, who kindly supplied rock samples, thin sections, and unpublished data.

Many thanks are due to P. DA ROIT, A. GIARETTA and G. MEZZACASA, who carried out the chemical and microprobe analyses.

Financial support from the C.N.R. (Centro Studi Orogeno Alpi Orientali, Padova) and the M.P.I. is also acknowledged.

REFERENCES

- BELLIENI G., MOLIN G.M., VISONÀ D. (1979) - *The petrogenetic significance of the garnets in the intrusive massifs of Bressanone and Vedrette di Ries (Eastern Alps-Italy)*. N. Jb. Miner. Abh., 136, 238-253.
- BÖGEL H., MORTEANI G., SASSI F.P., SATIR M., SCHMIDT K. (1979) - *The Hercynian and pre-Hercynian development of the Eastern Alps. Report on a meeting*. N. Jb. Geol. Pal. Abh., 159, 97-112.
- BURRI C. (1959) - *Petrochemische Berechnungsmethoden auf äquivalenter Grundlage (Methoden von Paul Niggly)*. Birkhäuser Verlag, Basel.
- CARDIN A., PISANI F., SASSI F.P., VISONÀ D., ZIRPOLI G. (1984) - *Nuovi dati sul basamento sudalpino in Val Sarentino (Alpi Orientali)* (in prep.).

- CONTINI R., SASSI F.P. (1980) - *Su alcuni effetti metamorfici alpini nel basamento austridico in Pusteria (Alpi Orientali)*. Mem. Ist. Geol. Miner. Univ. Padova, 34, 187-194.
- FAZEKAS V., KOSA L., SELMECZI B. (1975) - *Rare earth mineralization in the crystalline schists of the Sopron Mountains*. Földtani Közöly, 105, 297-308.
- GOMEZ-PUGNAIRE M.T., SASSI F.P. (1983) - *Pre-Alpine metamorphic features and alpine overprints in some parts of the Nevado-Filabride basement (Betic Cordilleres, Spain)*. Mem. Ist. Geol. Miner. Univ. Padova, 36, 49-72.
- GREEN T.H. (1977) - *Garnet in silicic liquids and its possible use as a P-T indicator*. Contr. Min. Petrol., 18, 163-174.
- KISHAZI P. (1977) - *A contribution to the knowledge of metamorphic rocks of Sopron Hills (Western Hungary)*. Verh. Geol. B.-A., Wien, pp. 35-43.
- KISHAZI P., IVANCSICS J. (1976) - *The metamorphic rocks of Western Hungary* (in hung. manuscript).
- KOSA L. (1976) - *The geology of the Fertőrákos metamorphic complex*. Ph. D. Thesis, Budapest.
- KOSA L., FAZEKAS V. (1981) - *Geologisch-petrographischer Aufbau des kristallinen Schieferkomplexes von Fertőrákos (Sopron Gebirge, West-Ungarn)*. Földtani Közöly, 111, 424-443.
- KOVÁCH A., SVINGOR E. (1981) - *On the age of metamorphism in the Fertőrákos metamorphic complex, W. Hungary*. Verh. Geol. B.A. Wien, 73-81.
- KUNO M. (1968) - *Differentiation of basalt magmas*. Wiley Intersciences publ., New York, 624-688.
- LEAKE B.E. (1964) - *The chemical distinction between ortho- and para-amphibolites*. Journ. Petr., 5, 238-254.
- LEAKE B.E. (1978) - *Nomenclature of amphibolites*. Canad. Mineralogist, 16, 501-520.
- LELKES-FELVÁRI Gy., SASSI F.P. (1981) - *Outlines of the pre-Alpine metamorphisms in Hungary*. IGCP Project No. 5, Newsletter, 3, 89-99. Karamata S. & Sassi F.P. eds.
- LELKES-FELVÁRI Gy., SASSI F.P., VISONÀ D. (1983) - *On the genesis of some leuchtenbergite-bearing metamorphic rocks and their phase relations*. Rendiconti Soc. It. di Min. Petr., 38 (2), 607-615.
- MIELKE P., WINKLER H.G.F. (1979) - *Eine bessere Berechnung der Mesonorm für granitische Gesteine*. N. Jb. Miner. Mh., 10, 471-481.
- SASSI F.P., SCHÖNLAUB H.P., ZANFERRARI A. (1978) - *The pre-Variscan history of the Eastern Alps*. Österr. Akad. Wiss., 3, 261-277.
- SASSI F.P., HAIDUTOV I., GOMEZ-PUGNAIRE M.T. (1979) - *Metamorphic correlation within the ambit of IGCP project No. 5: problems, present status, and next steps*. In: SASSI F.P. ed., IGCP No. 5, Newsletter, 103-110.
- SASSI F.P., ZIRPOLI G. (1979) - *Stato delle conoscenze sulla storia pre-ercinica delle Alpi Orientali*. Mem. Soc. Geol. Ital., 20, 11-20.
- SASSI F.P., BELLINI G., PECCERILLO A., POLI G. (1980) - *Some constraints on geodynamic models in the Eastern Alps*. N. Jb. Geol. Pal. Mh., 707-718.
- SASSI F.P., ZANETTIN B., ZIRPOLI G. (1980 b) - *Quadro della storia termica alpina nelle Alpi orientali*. Rend. Soc. Ital. Min. Petr., 36, 19-33.
- SASSI F.P., SCHMIDT K. (1982) - *The «Caledonian» event in the Eastern Alps: Guide-lines of its geodynamic interpretation*. SASSI F.P. & VARGA I. (Eds.), IGCP No. 5, Newsletter, 4, 78-81.
- SURYA F. (1971) - *Chemical distinction of high grade ortho- and parametabasites*. Norsk. Geol. Tidsskr., 51/3, 311-316.
- VENDEL M. (1973) - *Skizze des geologischen Aufbaues der Stadt Sopron und ihrer Umgebung (W-Ungarn)*. Ung. Geol. Anstalt Budapest, 1-28.
- VENDEL M., KISHAZI P., BOLDIZSÁR I. (1974) - *The crystalline schists of the Sopron Mts.* (in hung. manuscript).
- WINKLER H.G.F., BREITBART R. (1978) - *New aspects of granitic magmas*. N. Jb. Miner. Mh., 10, 463-480.